Quantification of net uplift and erosion on the Norwegian Shelf south of 66°N from sonic transit times of shale

SVEN HANSEN

Hansen, S.: Quantification of net uplift and erosion on the Norwegian Shelf south of 66°N from sonic transit times of shale. *Norsk Geologisk Tidsskrift*, Vol. 76, pp. 245–252. Oslo 1996. ISSN 0029-196X.

A relationship between burial depth and sonic interval transit times has been established for normally compacted Upper Jurassic to Tertiary shale intervals from 32 carefully selected Norwegian Shelf wells located between the Danish–Norwegian sector border and 66°N. The normal shale interval transit time trend is expressed as $\Delta t = 191 \exp(-0.00027z)$, where Δt is the shale transit time (μs/ft) and z is burial depth in metres. During the late Cenozoic, mainland Norway and the eastern part of the Norwegian Shelf experienced uplift and erosion, which resulted in shale over-compaction. Twenty-nine wells were identified as being located within the uplifted area south of 66°N, and the established normal interval transit time trend was used to quantify magnitudes of net uplift and erosion from shale intervals in each well. The average standard deviation of the quantification was 260 m and the maximum magnitude of net uplift and erosion determined in the wells was 610 m. The late Cenozoic uplift hinge-line is sub-parallel to the present-day Norwegian coastline, as are the iso-uplift curves whose magnitudes increase landwards. Compared to earlier studies, the magnitudes presented here differ slightly from those of other workers, probably because of the different methods employed.

Sven Hansen, Geologisk Institut, Aarhus Universitet, DK-8000 Århus C, Denmark.

Introduction

The widely recognized uplift of mainland Norway and its adjacent offshore basins has traditionally been explained by geomorphologists as arising from isostatic uplift of Fennoscandia, due to unloading after the end of the Quaternary glaciations (Reusch 1901; Nansen 1921; Grønlie 1922). Today it is recognized that several other factors were involved which were probably more important than deglaciation. It has been suggested that the uplift was related to the opening of the Atlantic Ocean and the associated perpherical bulge affecting the Atlantic Ocean margins (Torske 1972; Sales 1992). The uplift has been observed in England, East Greenland and Scandinavia (Bulat & Stoker 1987; Green 1989; Rundberg 1989; Hillis 1991, 1993; Christiansen et al. 1992; Doré 1992; Ghazi 1992; Japsen 1992; Jensen & Michelsen 1992; Jensen & Schmidt 1992; Nyland et al. 1992; Riis & Fjeldskaar 1992; Richardsen, Vorren & Tørudbakken 1993; Stuevold & Eldholm 1996). For more information concerning the geological history of the North Sea, see Glennie (1990).

The importance of accurately quantifying the magnitude of uplift relates to its effect on seals, reservoirs and source rocks (as detailed by Doré & Jensen 1996). Examples of studies attempting to do this include: Stuevold & Eldholm (1996) who used volumetric considerations of the erosion between 62° and 68°N; Ghazi (1992), who estimated erosion in the Stord Basin (between 59° and 60°N) by comparing thicknesses of Mio-Pliocene sediments in surrounding wells with those interpreted from seismic sections; and Jensen & Schmidt (1992), who used seismic profiles, vitrinite reflectance data and shale compaction in the Skagerrak area (between approximately 56°N and 58°N). A map showing a general overview of late Cenozoic uplift is given by Doré & Jensen (1996; their Fig. 2).

Our study area embraces those of these other workers and stretches from the Danish–Norwegian sector border to 66°N (Fig. 1). Furthermore, we quantified magnitudes of net uplift and erosion using a single method – based on a normal shale compaction trend established from sonic internval transit times of shale intervals in several wells. Only the magnitudes of the latest episode of uplift can potentially be quantified in this way, as earlier episodes do not normally influence the determinations (as explained below).

Determination of the magnitude of net uplift and erosion from shale compaction

If the permeability of the rocks permits the pore pressure to be hydrostatic (i.e. no over-pressure development), porosity decreases systematically with increasing burial depth – i.e. normal compaction (Athy 1930; Magara 1980; Sclater & Christie 1980; Baldwin & Butler 1985; Dzevanshir, Buryakovskiy & Chilingarian 1986; Huang & Gradstein 1990). The basic assumption underlying the quantification of uplift from shale compaction is that the process is irreversible. A shale will thus retain the

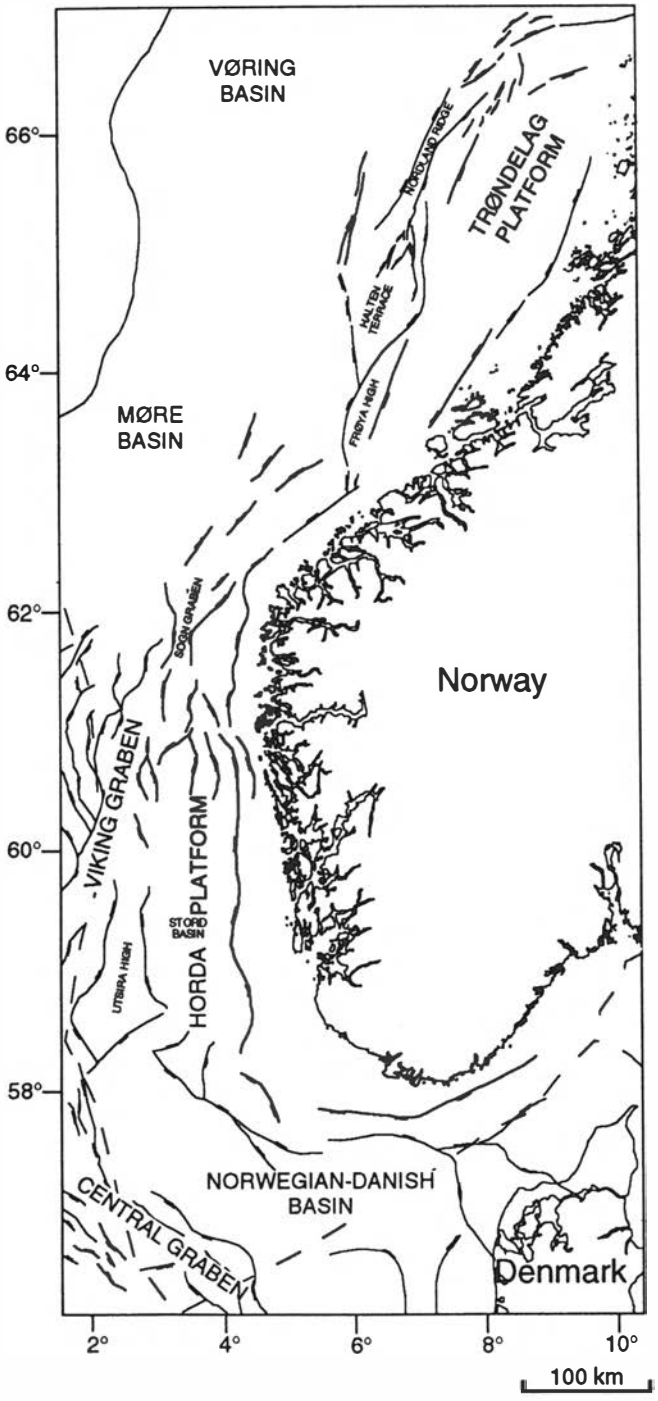

Fig. 1. Main structural elements of the study area.

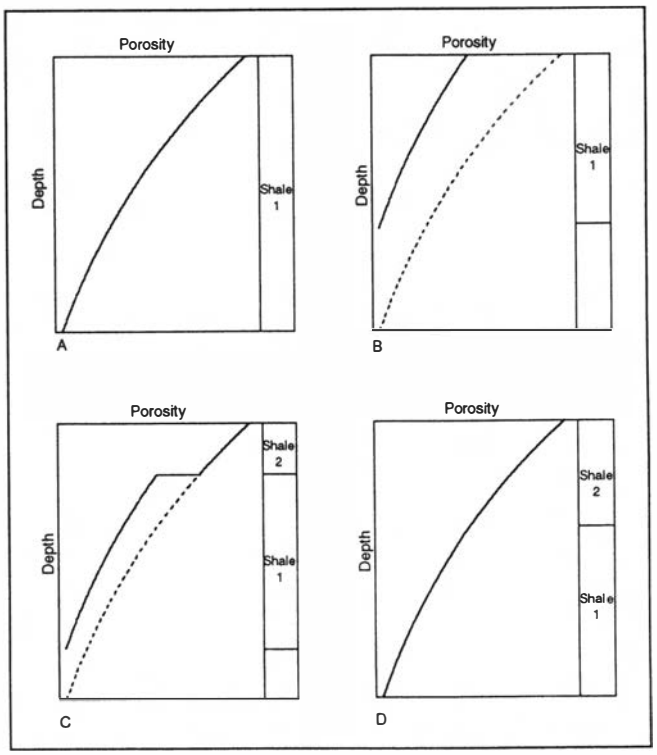

Fig. 2. Porosity trends for two shale sequences subjected to subsidence and deposition, uplift and erosion and continued subsidence and deposition. A – Porosity trend for Shale 1 after deposition and normal compaction. B – Shale 1 has been uplifted and partly eroded, leading to shale porosities (solid curve) being lower than those indicated by the normal compaction trend (stippled curve); Shale 1 thus appears to be over-compacted. C – Subsidence has recommenced and a new shale sequence (Shale 2) has been deposited on top of Shale 1. Shale 1 still appears to be over-compacted, but not as much as in B. D – The thickness of Shale 2 equals that of the eroded thickness of Shale 1, which means that Shale 1 no longer appears as over-compacted.

compaction it has gained at maximum burial depth. If uplift and erosion take place, a shale will have lower porosities than those anticipated from its present burial depth, i.e. the shale will appear as over-compacted.

Fig. 2 shows the hypothetical burial history of two shale sequences (Shale 1 and Shale 2). A normal porosity trend for Shale is shown in Fig. 2A, while in Fig. 2B the sequence has been uplifted and partly eroded. Compared to the normal compaction trend (the stippled curve), Shale 1 now appears as over-compacted (Fig. 2B). In Fig. 2C, subsidence has recommenced and a second, normally compacted shale sequence (Shale 2) has been deposited on top of the overcompacted sequence (Shale 1). Over-compaction (the horizontal distance from the normal compaction trend) is now smaller than that in Fig. 2B. In Fig. 2D, the originally uplifted and eroded shale sequence (Shale 1) has been buried to a depth equal to the original maximum burial depth, and the sequence no longer appears as over-compacted. Below this depth, the porosity of the shale sequence which experienced uplift (Shale 1) will continue to be reduced along the normal compaction trend. In summary: the determination of apparent uplift from shale compaction will only yield a true magnitude in scenario 2B; a magnitude less than the actual value will be obtained in scenario 2C; and in scenario 2D; uplift cannot be recognized at all.

Using the shale compaction method for determination of uplift and erosion will therefore *not* yield the original magnitudes of uplift (unless no sediment has been deposited after erosion), but the *differences* between the present and maximum burial depth (defined as net uplift by Nyland et al. 1992; Jensen & Schmidt 1993). *Net uplift and erosion* was therefore used in this study as quantification of net uplift based on shale compaction requires that the overburden has been reduced by erosion. Recall that it is important to keep in mind that when an earlier

uplifted and eroded shale sequence is buried beneath a younger sequence which is equal or greater in thickness to the eroded sediments, the original sequence will appear as normally compacted: this means that only the magnitude of the latest episode can be quantified.

Establishment of a normal shale compaction trend is essential for quantifying the magnitude of net uplift and erosion from shale compaction. It is also important that the method is based on a trend specifically established for the area under investigation, as a comparison of shale compaction trends shows that they differ from basin to basin (see Rieke & Chillingarian 1974; Hermanrud 1993).

The amount of data normally available from petrophysical well logs potentially facilitates the use of a porosity-related well log parameter for this purpose, such as the interval transit time (inverse of velocity) from the sonic log, bulk density from the density log, or neutron porosity from the neutron log. However, as neutron porosities measured in shale intervals are only slightly influenced by compaction (Rider 1986) this log cannot be used. Furthermore, the reduction of vertical stress experienced during uplift and erosion may result in the fracturing of the uplifted rocks. The acoustic waves transmitted by the sonic tool avoid such fractures and are mainly influenced by the intergranual porosity, whereas the density log is influenced both by intergranular *and* fracture porosity (Rider 1986). It is therefore likely that interval transit time will yield more reliable results than bulk density: the sonic log is also less influenced by borehole effects and is commonly run over wider intervals than the density log. For these reasons, it was decided to establish a normal interval transit time as the basis for quantifying net uplift and erosion on the Norwegian Shelf.

Transit time and shale compaction

Magara (1976) proposed the following exponential relationship between transit time and burial depth for shales with hydrostatic pore pressure:

$$\Delta t = \Delta t_0 \exp(-cz) \quad (1)$$

where Δt is transit time measured by the sonic log, Δt_0 is the transit time at the present sedimentary surface, c is the compaction coefficient and z is the present burial depth. For normally compacted shales, the value of Δt_0 will be the same as that of water (Magara 1976) which is somewhere between 185 μs/ft and 189 μs/ft depending on salinity (Schlumberger 1989). Magara (1976), however, used a value of $\Delta t_0 = 200$ μs/ft, which is probably too high. For over-compacted shales, Δt_0 is lower than the transit time of water (Fig. 3). If the pore pressure is greater than hydrostatic, a shale may have higher porosities and interval transit times than a normally compacted shale at the same burial depth (Fig. 3); i.e. the shale is under-compacted. Usually there is no simple relationship between burial depth and transit time or porosity for under-compacted shales.

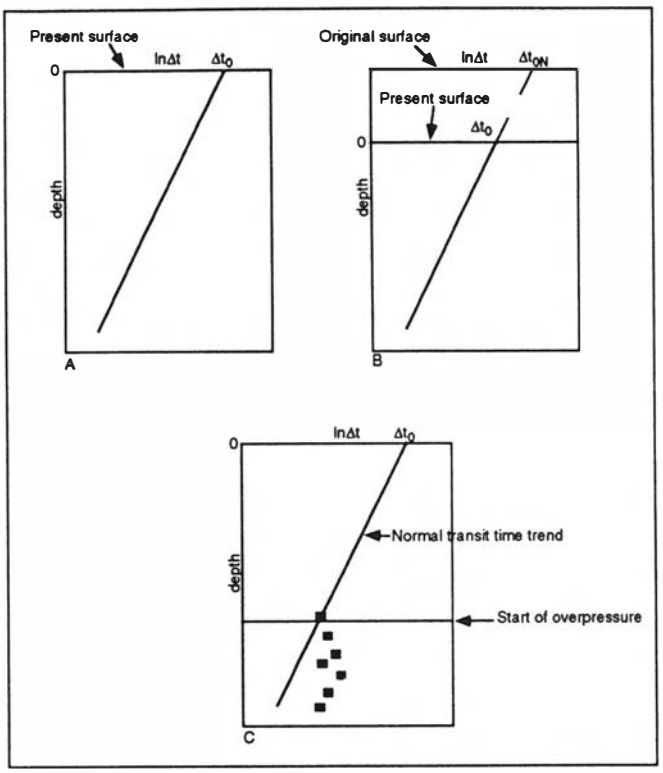

Fig. 3. A – The interval transit time trend for a normally compacted shale is a straight line on a log-normal diagram and Δt_0 is close to the interval transit time of water. B – Erosion has removed the uppermost sediments. The transit time at the surface (Δt_0) is lower than that of a normally compacted shale (Δt_{0N}). C – Over-pressure may result in higher porosities and thus higher interval transit times than a normally compacted shale (under-compaction). Under-compaction can be recognized as a deviation of the interval transit times from the normal transit time trend (modified from Magara, 1976).

By rearranging equation 1 the maximum burial depth (z_{max}) can be calculated as:

$$z_{max} = \ln(\Delta t/\Delta t_{0N})/(-c) \quad (2)$$

and the net uplift and erosion (Δz) is calculated by subtracting the present burial depth (z)

$$\Delta z = \ln(\Delta t/\Delta t_{0N})/(-c) - z \quad (3)$$

where Δt_{0N} is the value of Δt_0 for normally compacted shales.

The normal transit time trend for the study area

Shale intervals in 151 wells on the Norwegian Shelf in the study area were identified using the gamma-ray log, the neutron-density separation, and lithologic data from completion logs.

When establishing a normal transit time trend, sections containing over-pressured shales in each well must be identified and excluded. Pore pressure evaluations from completion reports were used for this. North of 64°N, all of the investigated Tertiary and Cretaceous shales are over pressured, probably as a result of high Pliocene and Pleistocene sedimentation rates. In only 11 of the investigated wells did shale intervals of Jurassic age have hydrostatic pore pressures (Tables 1 and 2). South of 62°N

Table 1. The 32 wells used to establish the normal transit time trend, together with the shale depth intervals from which the interval transit time were taken and their chronostratigraphy. n = the number of shale transit time values from each well.

Well	Burial depth (m)	Chronostratigraphy	n
3/5-1	421–1521	Miocene–Oligocene	111
3/5-2	418–1398	Miocene–Oligocene	99
8/1-1	472–2592	Miocene–Jurassic	65
8/3-1	334–1744	Miocene–Jurassic	113
8/3-2	360–1890	Miocene–L. Cretaceous	104
8/4-1	343–2303	Miocene–Jurassic	74
8/12-1	643–1663	Miocene–Oligocene	92
9/4-2	551–2391	Miocene–L. Cretaceous	110
16/7-5	683–1333	Miocene–Oligocene	59
17/4-1	318–2138	Miocene–Jurassic	51
17/10-1	515–2865	Miocene–Jurassic	170
17/11-1	458–2288	Miocene–Jurassic	133
17/11-2	448–2278	Miocene–L. Cretaceous	106
17/12-2	807–2087	Oligocene–L. Cretaceous	76
17/12-3	374–2054	Miocene–L. Cretaceous	108
25/6-1	2053–2133	Paleocene	109
25/8-2	589–2409	Miocene–Jurassic	80
26/4-1	2186–2826	U. Cretaceous–Jurassic	59
30/4-1	2125–2345	Paleocene–U. Cretaceous	23
30/6-14	2359–2729	Jurassic	38
30/9-5	2092–2842	Paleocene–Jurassic	59
31/4-2	1883–2023	U. Cretaceous–Jurassic	15
31/4-3	1785–1805	Paleocene	3
31/4-4	1841–2131	U. Cretaceous–Jurassic	28
31/4-5	1882–1922	L. Cretaceous–Jurassic	5
31/4-6	1915–1955	U. Cretaceous	4
31/4-7	1829–1929	U. Cretaceous–Jurassic	11
31/4-8	1901–2421	Jurassic	43
34/8-3	915–1135	Oligocene–Eocene	12
34/10-30	802–1282	Oligocene–Eocene	27
6607/12-1	850–980	Miocene–Oligocene	12
6609/11-1	997–2017	Miocene–Jurassic	96
Total			2095

Table 2. The 29 wells in which the shales were identified as being over-compacted and the 3 wells identified as containing normally compacted shales (net uplift and erosion is 0 m) but not used to establish the normal transit time trend, together with estimated magnitudes of net uplift and erosion. STD = the standard deviation of net uplift and erosion estimates; n = the number of shale transit time values used in the calculations.

Well	Net uplift and erosion	STD	n
9/2-1	390	231	108
9/2-2	235	176	115
9/4-1	95	209	114
9/4-3	160	329	63
9/4-4	190	212	77
9/8-1	180	224	114
9/10-1	0	207	114
9/11-1	165	237	112
9/12-1	260	255	128
10/5-1	400	268	49
10/7-1	350	105	18
11/10-1	320	206	89
18/11-1	560	261	81
31/6-1	450	168	46
31/6-6	400	168	46
35/11-1	250	204	48
35/11-2	75	261	96
35/11-3	110	191	128
35/3-5	190	329	180
35/8-1	30	299	216
35/8-2	95	365	186
35/8-3	70	185	178
35/9-1	610	313	58
36/1-1	430	278	51
36/1-2	120	265	152
6205/3-1	340	116	81
6305/12-1	100	310	180
6306/10-1	485	215	169
6407/1-3	0	334	130
6407/10-1	225	104	11
6407/6-4	230	388	53
6507/12-3	0	314	12
Total		260	3291

the over-pressured shales are mainly encountered in wells in the Viking Graben and the Central Trough.

Sixty-six of the investigated wells contain shale intervals with hydrostatic pore pressures. Δt_0 was determined in each of them by fitting equation 1 to the interval transity times using linear regression. Wells with normally compacted and over-compacted shales were identified using the calculated values of Δt_0. Fig. 4 illustrates two wells whose shales are identified as being normally compacted (9/4-2, $\Delta t_0 = 188\ \mu s/ft$) and over-compacted (9/2-2, $\Delta t_0 = 166\ \mu s/ft$), respectively. In 32 wells the shales were identified as being normally compacted, while 29 wells contain shales identified as being over-compacted. Three other wells contain normally compacted shale intervals, but they were rejected as they lie very close to the uplift hinge-line. All wells are listed in Tables 1 and 2 and their locations are shown on Fig. 5.

The normal interval transit time trend for shales on the Norwegian Shelf was thus established from the transit times (averaged over 10 m intervals) in the 32 wells containing normally compacted shales. An exponential relation between depth and interval transit time (determined from standard regression methods, Fig. 6) and emerged as:

$$\Delta t = 191 \exp(-0.00027z) \quad (4)$$

where z is the burial depth in metres and Δt at the interval transit time in $\mu s/ft$. The regression correlation coefficient is 0.91 and the determined value of Δt_{0N} (191 $\mu s/ft$) is very close to that of water (185–189 $\mu s/ft$). An expression for determining Δz was established by rearranging equation 4 and subtracting the present burial depth (z):

$$\Delta z = \ln(\Delta t/191)/(-0.00027) - z \quad (5)$$

Results and discussion

Equation 5 was used to determine the magnitude of the late Cenozoic net uplift and erosion in the 29 over-compacted wells (Table 2). Figs. 4B and D show the frequency distribution of Δz calculated from shale transit times in well 9/4-2 and 9/2-2. The shales in well 9/4-2 were identified as being normally compacted and the distribution of Δz show an almost normal distribution

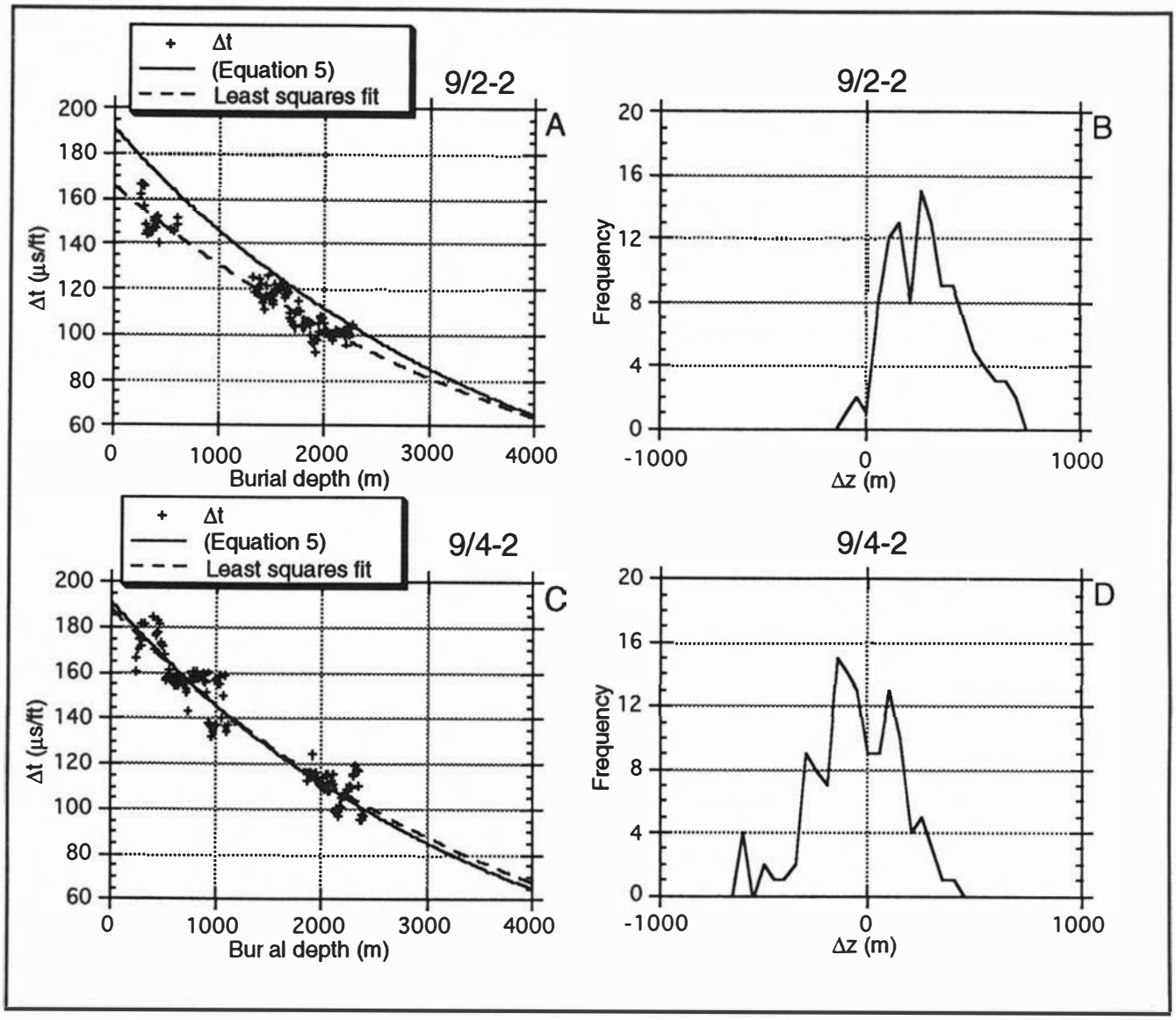

Fig. 4. A – Shale interval transit times from well 9/2-2 versus depth. The least square fit is: $166 \exp(-0.000255z)$ where z is in metres, R = 0.96. B – The frequency distribution of Δz determined from the shale transit times in well 9/2-2. C – Shale interval transit times from well 9/4-2 vs. depth. The least square fit is: $188 \exp(-0.000239z)$ where z is in metres, R = 0.96. D – The frequency distribution of Δz determined from the shale transit times in well 9/4-2.

around 0 m. The values of Δz calculated for the shale intervals in well 9/2-2 are distributed around a value which is clearly higher than 0 m. The median of the calculated values of Δz was used as the estimate of net uplift and erosion for this well. The standard deviation of the determination of the magnitude of net uplift and erosion in the wells is between 105 and 405 m (Table 2). The average standard deviation of the detemination of net uplift and erosion is 260 m using the method applied in this study. This is slightly less accurate than previously estimated by Statoil. Statoil has regarded the precision of the method to be ±200 m (Skagen 1992). The shale compaction methods seems to be slightly less accurate than the vitrinite reflection method (±200 m) but more accurate than estimates based on the opal-CT transition (±500 m), the crystallinity index of illite (±500 m) and apatite fission track analysis (±500–1000 m) (Skagen 1992).

The iso-uplift curves were constructed by (i) grouping the wells into four classes based on the determined magnitudes of net uplift and erosion (0–200 m, 200–400 m, 400–600 m, and >600 m and (ii) placing the iso-uplift curves between the areas where these groups are located. This method was used because the error involved in determining the net uplift and erosion does not justify greater precision.

As only a few wells north of 62°N were available for quantification (due to over-pressure in most of the shale intervals), the determination of iso-uplift curves in this area is less accurate. The hinge line is located east of the Nordland Ridge (Stuevold & Eldholm 1996) where there is no evidence for late Cenozoic uplift and erosion (Goll & Hansen 1992). Both the hinge line and iso-uplift curves have a SW–NE trend running sub-parellel to the coast. The maximum of the determined values of net

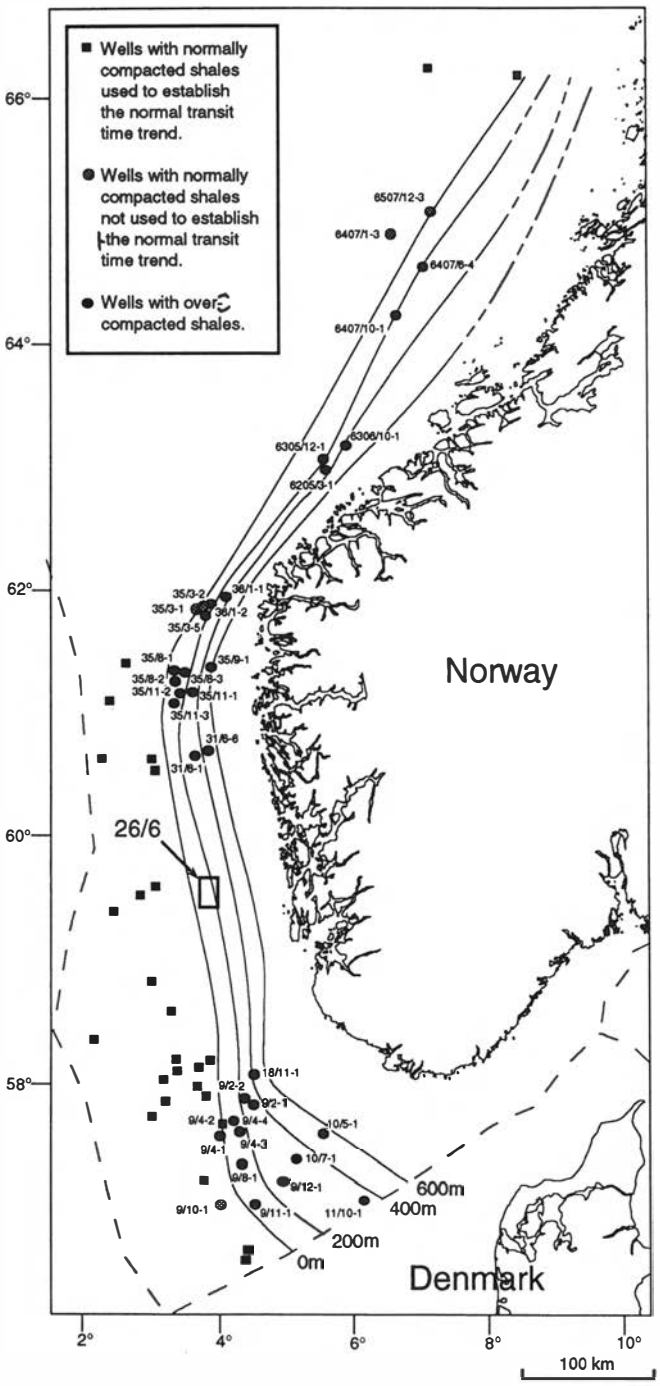

Fig. 5. Well locations and iso-uplift curves (in metres) for quantified net uplift and erosion. Well numbers are given for wells with over-compacted shale intervals.

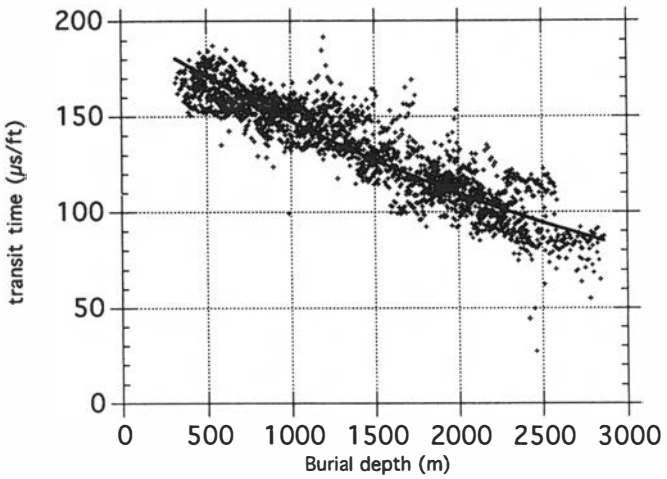

Fig. 6. Interval transit times for normally compacted shales in wells identified as being located in the area without net uplift. These were used to establish a normal transit time trend (eq. 4) for shales at the Norwegian Margin.

uplift and erosion is 485 m in well 6306/10-1. Well 6306/10-1 is located approximately 50 km northwest of the present Norwegian coast. Since the uplife increases towards the coast it seems likely that close to the present-day Norwegian coast-line the magnitude is 500 m or more. Stuevold & Eldholm (1996) estimated tectonic uplift near the present-day Norwegian coast to be about 1000 m north of 65°N and 500 m or less south of 65°N. Although our data conform to their estimate north of 65°N, uplift to the south seems to have been greater than 500 m, as indicated by well 6306/10-1. Stuevold & Eldholm (1996) also interpreted the hinge line south of 66°N as having a N–S trend, while this study indicates a SW–NE trend. However, the available data north of 64°N are limited and the magnitude of the uplift and erosion must therefore be interpreted with caution.

Wells 35/3-1, 2 and 5, and 36/1-1 and 2 occur at the transition between the area north of 62°N (where the iso-uplift curves trend NE–SW) and the area between 58°N and 62°N (where they trend N–S). This transition zone is located where the shelf is relatively narrow and the magnitudes of net uplift and erosion show a considerable landward increase over a relatively short distance from the hinge line.

The maximum amount of net uplift and erosion between 58°N and 62°N is 610 m in well 35/9-1. Based on seismic evidence, Rundberg (1989) recognized – but did not quantify – Pliocene uplift and erosion between 60°N and 62°N. Fig. 7 shows the age and seismically mapped distribution of sediments sub-cropping the mid-Pliocene unconformity from Rundberg (1989), together with determinations of net uplift and erosion derived from this study. This reveals that the magnitudes change according to the location of the wells with respects to the sub-crop distribution; 0–100 m in the area of the Early Pliocene sub-crop; 100–200 m in the area of the Miocene and Oligocene sub-crops; 400–500 m in the area of Eocene sub-crop; and 610 m (well 35/9-1) in the area of the Paleocene sub-crop.

The only exceptions to this trend are wells 31/6-1 and 35/11-1, where the values are 450 m and 250 m, respectively. As well 31/6-1 is located where Late Eocene/Early Oligocene sediments sub-crop the mid Pliocene unconformity, the magnitude would be expected to be somewhere between 200 m and 400 m based on observations from the other wells. As the standard deviation for this well is 402 m, the figure of 450 m may very well be too high and may indeed lie somewhere within the expected

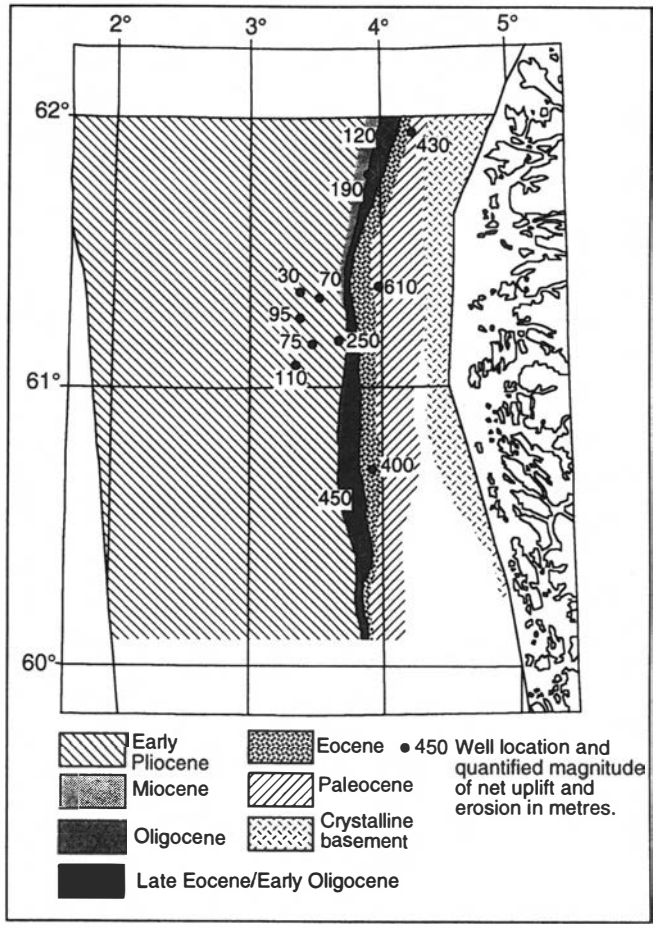

Fig. 7. Map showing the age of sediments sub-cropping the mid-Pliocene unconformity mapped by Rundberg (1989) with superimposed magnitudes of net uplift and erosion quantified in this study.

range. For well 35/11-1, which is located where Early Pliocene sediments sub-crop the mid-Pliocene unconformity (and lies very close the area where Oligocene and Late Eocene/Late Oligocene sediments sub-crop), the magnitude of net uplift and erosion would be expected to be less than 200 m. With a standard deviation of 204 m for well 35/11-1, it is possible that the value is overestimated by some 50–100 m.

No wells have been drilled between 59°N and 60°N in the area where net uplift and erosion is supposed to have taken place. From observed thicknesses in surrounding wells and interpreted thicknesses from seismic sections, Ghazi (1992) estimated that 400–600 m of Mio-Pliocene sediments have been removed as a result of late Cenozoic uplift in the central part of the Stord Basin in block 26/6 (Fig. 5). Due to the lack of wells in this area net uplift and erosion has been estimated to be between 200 and 400 m by connecting the iso-uplift curves north of 60°N to those south of 59°N. The substantial difference between our result and that of Ghazi probably arises from the different methods used. Ghazi's estimate relates solely to late Cenozoic erosion. Sediments were subsequently deposited upon the eroded sequence thus making the calculated net uplift and erosion lower than the amount of erosion which actually took place (as illustrated in Fig. 2).

South of 58°N, the iso-uplift curves (of this study) trend NW–SE (Fig. 5). The maximum amounts of net uplift and erosion are 560 m in well 18/11-1 and 400 m in well 10/5-1. In this area Jensen & Schmidt (1992) produced their magnitudes on the basis of shale compaction, vitrinite reflectance and seismic profiles. They did not, however, establish a normal shale compaction curve but used that of Sclater & Christie (1980) (Jensen pers. comm.) to quantify the magnitude of the net uplift and erosion. Jensen & Schmidt's (1992) suggestion that wells 9/4-1 and 9/4-2 are very close to the uplift hinge line agrees with our results. Furthermore, they identified well 9/8-1 as being close to the hinge line and suggested that well 9/11-1 was beyond the area of net uplift and erosion. Using our method, it was found that the magnitudes of net uplift and erosion in these wells are 180 m and 165 m, respectively. Based on this, we suggest that the hinge line should be located slightly to the SW of that of Jensen & Schmidt (1992). The only other difference between the two studies is that wells 11/10-1 and 10/5-1 according to Jensen & Schmidt (1992; their Fig. 1) have experienced net uplift and erosion greater than 500 m, while our results indicate magnitudes of 320 m and 400 m, respectively. The vitrinite reflectance data of Jensen & Schmidt (1992; their Fig. 3) indicate that these wells have experienced approximately 400 m net uplift and erosion, which seems to be consistent with out results. The consequence of this difference is that our iso-uplift curves have a more easterly trend than theirs (Jensen & Schmidt 1992; their Fig. 1).

To achieve as reliable results as possible, the quantification of net uplift and erosion should be based on a calibration curve (compaction trend) established specifically for the study area. The method presented in this study minimizes the number of possible errors introduced in the quantification. First, the quantification is based on a calibration curve established for the study area. Second, the net uplift and erosion is calculated direcly from the transit times of the sonic log without any other calculations being introduced, keeping the number of calculations at an absolute minimum.

Conclusions

A normal interval transit time for shales has been established on the basis of 32 carefully selected Norwegian Shelf wells located between the Danish–Norwegian sector border and 66°N. The trend is expressed as:

$$\Delta t = 191 \exp(-0.00027z)$$

where Δt is transit time in μs/ft and z is burial depth in metres. This trend was used to quantify the magnitudes of net uplift and erosion for 29 wells identified as being located in the area which experienced late Cenozoic uplift and erosion. The average standard deviation was

260 m which is slightly higher than previously estimated by Statoil (Skagen 1992). Differences between the magnitudes found here and those of earlier studies are minor and are ascribed to the use of different methods. The iso-uplift curves are sub-parallel to the present-day Norwegian coast-line and show increasing magnitudes landwards. The maximum estimate of net uplift and erosion in the studied wells is 610 m.

Acknowledgements. – I thank Den norske stats oljeselskab a.s. (Statoil) for providing financial support for this project, supplying data and giving permission to publish. Lars N. Jensen of Statoil and Professor Olaf Michelsen of Aarhus University are thanked for their comments to an earlier version of the manuscript. I also thank the three reviewers C. Hermanrud, A. G. Doré and B. Tørudbakken for improving the paper. Furthermore, I am grateful to Dr Antony Treverton Buller of Statoil for correcting the English.

Manuscript received May 1995

References

Athy, L. F. 1930: Density, porosity and compaction of sedimentary rocks. *American Association of Petroleum Geologists Bulletin 14*, 1–24.

Baldwin, B. & Butler, C. O. 1985: Compaction curves. *American Association of Petroleum Geologists Bulletin 69*, 622–626.

Bulat, J. & Stoker, S. J. 1987: Uplift determination from interval velocity studies, UK scuthern North Sea. *In* Brooks, J. & Glennie, K. (eds.): *Petroleum Geology of North West Europe*, 293–305. Graham & Trotman, London.

Christiansen, F. G., Larsen, H. C., Marcussen, C., Hansen, K., Krabbe, H., Larsen, L. M., Piasecki, S., Stemmerick, L. & Watt, W. S. 1992: Uplft study of the Jameson Land basic, East Greenland. *Norsk Geologisk Tidsskrift 72*, 291–294.

Doré, A. G. 1992: The Base Tertiary Surface of southern Norway and the northern North Sea. *Norsk Geologisk Tidsskrift 72*, 259–265.

Doré, A. G. & Jensen, L. N. 1996: The impact of Late Cenozoic uplift and erosion on hydrocarbon exploration. *Global and Planetary Change 321. Special Issue: Impact of glaciations on basin evolution: data and models from the Norwegian Margin and adjacent areas.*

Dzevanshir, R. D., Buryakovskiy, L. A. & Chilingarian, G. V. 1986: Simple quantitative evalution of porosity of argillaceous sediments at various depths of burial. *Sedimentary Geology 46*, 169–175.

Ghazi, S. A. 1992: Cenozoic uplift in the Stord Basin area and its consequences for exploration. *Norsk Geologisk Tidsskrift 72*, 285–290.

Glennie, K. W. (ed.) 1990: *Introduction to the Petroleum Geology of the North Sea.* Blackwell, London, 402 pp.

Goll, R. M. & Hansen, J. W. 1992: The Cenozoic sequence stratigraphy of the Halten Terrace and the Outer Vøring Plateau based on seismic and biostratigraphic data. *Norsk Geologisk Tidsskrift 72*, 295–299.

Green, P. F. 1989: Thermal and tectonic history of the East Midlands shelf (onshore UK) and surrounding regions assessed by apatite fission track analysis. *Journal of the Geological Society, London 146*, 755–773.

Grønlie, O. T. 1922: Strandlinjer, moræner og skjælforekomster. *Norges Geologiske Undersøkelse 94*, 1–39.

Hermanrud, C. 1993: Basin modelling techniques – an overview. *In* Doré A. G. et al. (eds.): *Basin Modelling: Advances and Applications. NPF Special Publication 3*, 1–34, Elsevier, Amsterdam.

Hillis, R. R. 1991: Chalk porosity and Tertiary uplift, Western Approaches Trough, SW UK and NW French continental shelves. *Journal of the Geological Society, London 148*, 669–679.

Hillis, R. R. 1993: Tertiary erosion magnitudes in the East Midlands Shelf, onshore UK. *Journal of the Geological Society, London 150*, 1047–1050.

Huang, Z. & Gradstein, F. M. 1990: Depth–porosity, relationship from deep sea sediments. *Scientific Drilling 1*, 157–162.

Japsen, P. 1992: Landhævningerne i Sen Kridt og Tertiær i det nordlige Danmark. *Dansk Geologisk Forening, Årsskrift for* 1990–91, 169–182.

Jensen, L. N. & Michelsen, O. 1992: Tertiær hævning og erosion i Skagerrak, Nordjylland og Kattegat. *Dansk Geologisk Forening, Årsskrift for 1990–91*, 159–168.

Jensen, L. N. & Schmidt, B. J. 1992: Late Tertiary uplift and erosion in the Skagerrak area: magnitude and consequences. *Norsk Geologisk Tidsskrift 72*, 275–279.

Jensen, L. N. & Schmidt, B. J. 1993: Neogene uplift and erosion in the Northeastern North Sea; magnitudes and consequences for hydrocarbon exploration in the Farsund Basin. *In* Spencer A. M. (ed.): *Generation, Accumulation and Production of Europe's Hydrocarbons III. Special Publication E.A.P.G. No. 3*, Berlin, Springer Verlag.

Magara, K. 1976: Thickness of removed sedimentary rocks, paleopore pressure, and paleotemperature, southwestern part of Western Canada Basin. *American Association of Petroleum Geologists Bulletin 60*, 554–565.

Magara, K. 1980: Comparison of porosity-depth relationships of shale and sandstone. *Journal of Petroleum Geology 3*, 175–185.

Nansen, F. 1921: The strandflat and isostacy. *Videnskabsselskabets Skrifter. I. Matematisk-Naturvidenskabelig Klasse, 11.*

Nyland, B., Jensen, L. N., Skagen, J., Skarpnes, O. & Vorren, T. 1992: Tertiary uplift and erosion in the Barents Sea; magnitude, timing and consequences. *In* Larsen, R. M. et al. (eds.): *Structural and Tectonic Modelling and Its Application to Petroleum Geology*, NPF Special Publication 1, Elsevier, Amsterdam, 153–162.

Reusch, H. 1901: Nogle bidrag til forstaaelsen af hvorledes Norges dale og fjelde er blevne til. *Norges Geologiske Undersøgelse 32*, 124–217.

Richardsen, G., Vorren, T. O. & Tørudbakken, B. O. 1993: Post-Early Cretaceous uplift and erosion in the southern Barents Sea: A discussion based on analysis of seismic interval velocities. *Norsk Geologisk Tidsskrift 73*, 3–20.

Rider, M. H. 1986: *The Geological Interpretation of Well Logs.* Blackie & Son Limited, London, 175 pp.

Rieke, H. H. III & Chilingarian, G. V. 1974: *Compaction of Argillaceous Sediments.* Developments in Sedimentology 16, Elsevier, Amsterdam, 424 pp.

Riis, F. & Fjeldskaar, W. 1992: On the magnitude of the Late Tertiary and Quaternary erosion and its significance for the uplift of Scandinavia and the Barents Sea. *In* Larsen, R. M. et al. (eds.): *Structural and Tectonic Modelling and Its Application to Petroleum Geology*, NPF Special Publication 1, Elsevier, Amsterdam. 163–185.

Rundberg, T. 1989: *Tertiary Sedimentary History and Basin Evolution of the Norwegian North Sea between 60°N and 62°N. An Integrated Approach.* Dr. Ing. thesis. University of Trondheim, Norway, 292 pp.

Sales, J. K. 1992: Uplift and subsidence of northwestern Europe: possible causes and influence on hydrocarbon productivity. *Norsk Geologisk Tidsskrift 72*, 253–258.

Schlumberger, 1989: *Log Interpretation Charts.* Schlumberger Educational Services, 152 pp.

Sclater, J. G. & Christie, P. A. F. 1980: Continental stretching: An explanation of the Post-Mid-Cretaceous subsidence of the Central North Sea Basin. *Journal of Geophysical Research 85*, 3711–3739.

Skagen, J. I. 1992: Methodology applied to uplift and erosion. *Norsk Geologisk Tidsskrift 72*, 307–311.

Stuevold, L. M. & Eldholm, O. 1996: Cenozoic uplift of Fennoscandia inferred from a study of the mid-Norwegian margin. *Global and Planetary Change 321. Special Issue: Impact of glaciations on basic evolution: data and models from the Norwegian margin and adjacent areas.*

Torske, T. 1972: Tertiary oblique uplift of Western Fennoscandia; crustal warping in connection with rifting and break-up of the Laurasian continent. *Norges Geologiske Undersøkelse 273*, 43–48.